

Electronic Supplementary Information

Synthesis and Electron-transfer Properties of Benzimidazole-functionalized Ruthenium Complexes for Highly Efficient Dye-sensitized Solar Cells

Wei-Kai Huang,^a Chi-Wen Cheng,^a Shu-Mei Chang,^b Yuan-Pern Lee,^a and Eric
Wei-Guang Diao^{*,a,c}

^a*Department of Applied Chemistry and Institute of Molecular Science, National Chiao
Tung University, Hsinchu 300, Taiwan*

^b*Institute of Organic and Polymeric Materials, National Taipei University of
Technology, Taipei 106, Taiwan*

^c*On sabbatical leave in Department of Chemistry, University of Copenhagen,
DK-2100 Copenhagen, Denmark*

* Corresponding author. diao@mail.nctu.edu.tw.

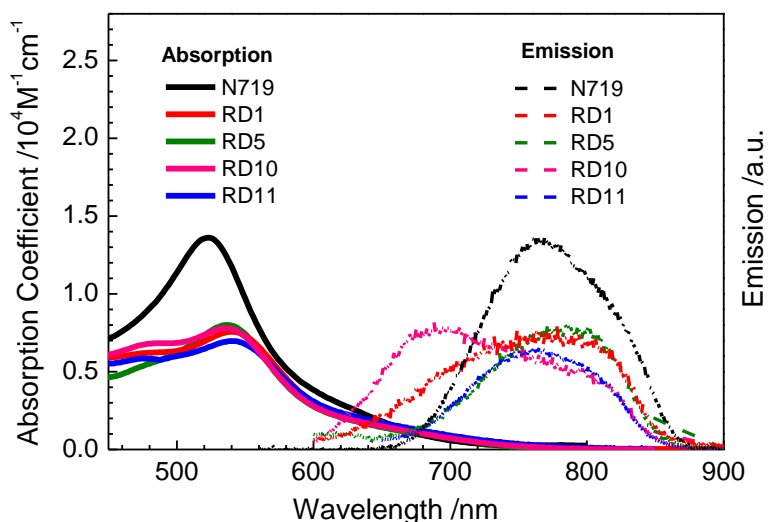


Figure S1. Absorption and emission spectra of (a) **RD1**, **RD5**, **RD10**, **RD11** and **N719** in DMF (2×10^{-5} M). The position of the intersection between the two spectra for each species determines the band gap energy E_{0-0} listed in Table S1.^{s1}

Table S1. Absorption coefficients ($\epsilon/\text{cm}^{-1}\text{M}^{-1}$), absorption maxima ($\lambda_{\text{max}}/\text{nm}$ between parentheses) and electrochemical data of **RD1**, **RD5**, **RD10**, **RD11** and **N719**

Dye	$\epsilon_{\pi-\pi^*}(\lambda_{\text{max}})$	$\epsilon_{\pi-\pi^*}$ or $\epsilon_{\text{MLCT}}(\lambda_{\text{max}})$	$\epsilon_{\text{MLCT}}(\lambda_{\text{max}})$	E_{ox}/V^a	E_{0-0}/V^b	$E_{\text{LUMO}}/\text{V}^c$
N719	49154 (310 nm)	13400 (384 nm)	13610 (524 nm)	0.97	1.85	-0.88
RD1	30704 (317 nm)	6324 (403 nm)	7560 (539 nm)	0.89	1.92	-1.03
RD5	28958 (315 nm)	5903 (388 nm)	8005 (537 nm)	0.90	1.86	-0.96
RD10	33710 (315 nm)	6393 (394 nm)	7796 (537 nm)	0.89	1.99	-1.10
RD11	22847 (313 nm)	6388 (388 nm)	6483 (538 nm)	0.79	1.85	-1.06

^a Oxidation potential E_{ox} (V vs F/Fc⁺) were measured for dyes in dry DMF in the presence of 0.1 M (*n*-C₄H₉)₄NPF₆ with a scan rate 50 mV s⁻¹ (vs NHE). ^b E_{0-0} was determined from the intersection of absorption and emission spectra^{s1} as shown in Figure S1. ^c E_{LUMO} was determined as $E_{\text{ox}} - E_{0-0}$.

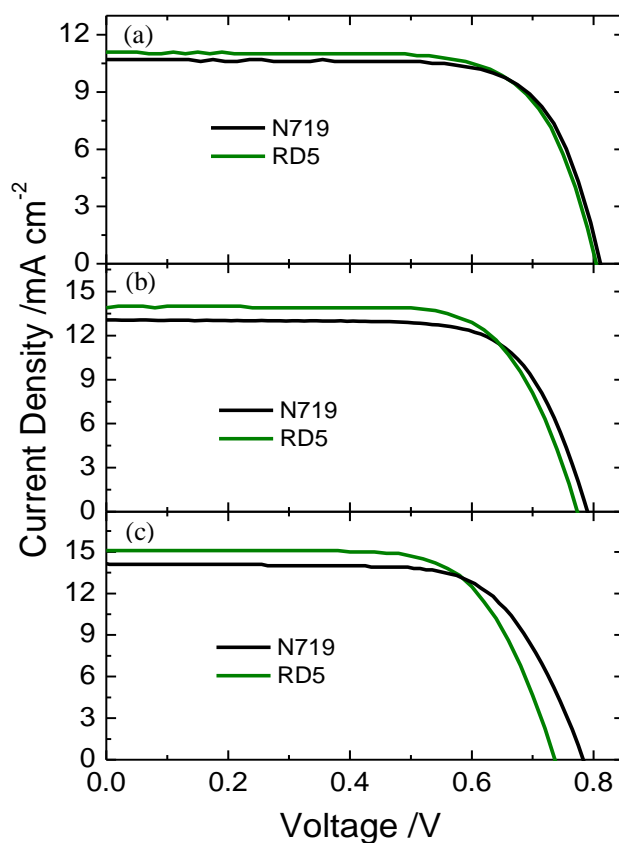


Figure S2. Current-voltage curves of **N719** and **RD5** with varied thickness of TiO₂ film (active layer + scattering layer): (a) (3+3) μm (b) (9+3) μm (c) (12+3) μm.

Table S2. Photovoltaic parameters of DSSC made of **N719** and **RD5** with three TiO₂ film thicknesses under simulated AM1.5 illumination (power 100 mW cm⁻²) and active area 0.16 cm²

TiO ₂ film Thickness	Dye	J_{sc} /mA cm ⁻²	V_{oc} /V	FF	η /%
3+3 μm	N719	10.656	0.810	0.74	6.4
	RD5	11.047	0.805	0.72	6.4
9+3 μm	N719	13.064	0.790	0.72	7.4
	RD5	13.947	0.773	0.72	7.8
12+3 μm	N719	14.157	0.783	0.70	7.8
	RD5	15.084	0.737	0.69	7.7

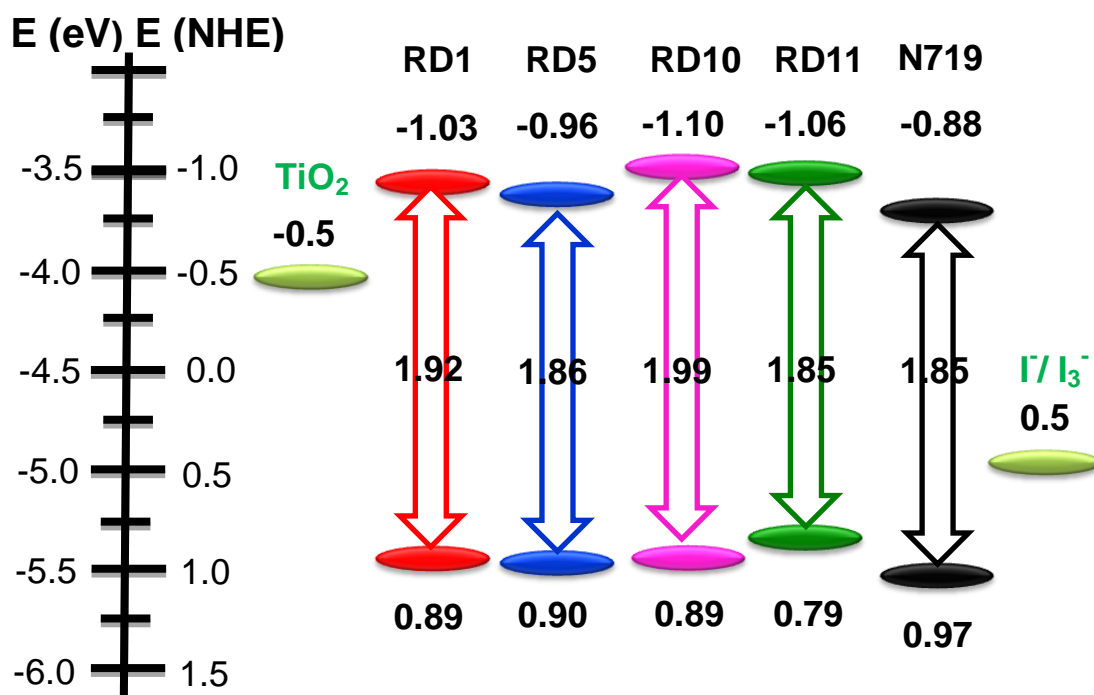
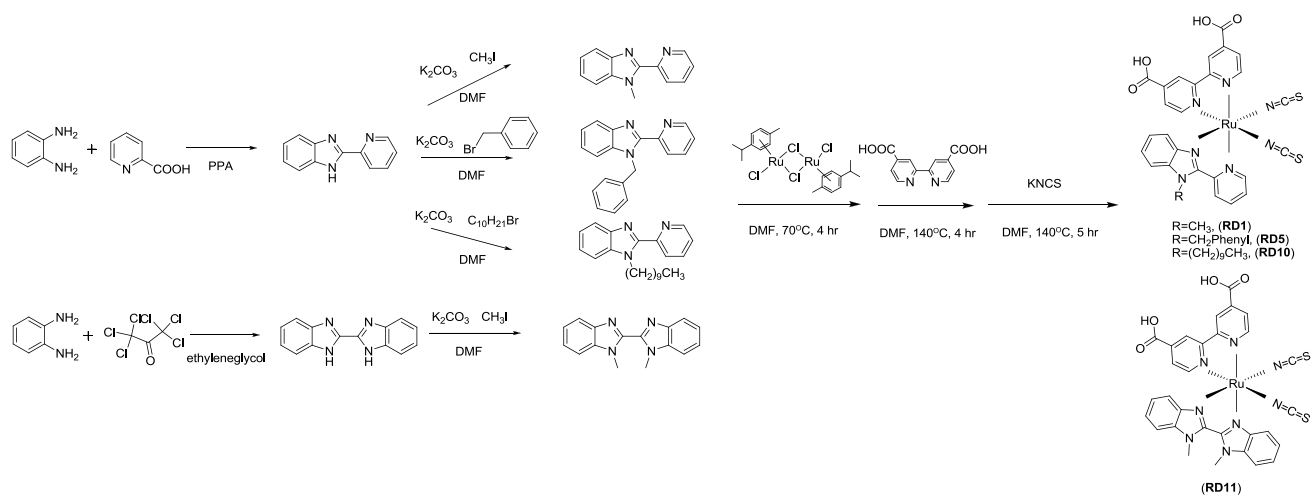


Figure S3. Schematic energies of **RD1**, **RD5**, **RD10**, **RD11** and **N719** showing the HOMO and LUMO levels obtained from electrochemical measurements (Table S1).

Synthesis of Ligands and Ruthenium Complexes

Scheme S1. Synthesis of RD ruthenium dyes



Ligands

2-(2-Pyridyl)benzimidazole (a)

Under an atmosphere of dinitrogen, picolinic acid (2.46 g, 0.02 mol), 1,2-benzenediamine (2.16 g, 0.02 mol) and PPA (10 g) were heated to 150 °C for 2 h. After cooling, the solution was poured into cool water with stirring; the pH was adjusted to 7-8 on addition of NaOH; the resulting gray/pink precipitate was filtered, washed with water, and dried in air. The crude product was purified on a column chromatograph (silica gel) with a mixture of ethyl acetate and hexane (1/1) as eluent (2.43 g, 62.0 %). ¹H-NMR (DMSO-d₆): 8.76 (d, J = 4.0 Hz, 1H), 8.31 (d, J = 7.6 Hz, 1H), 8.01 (ddd, J = 8.0, 8.0, 1.6 Hz, 1H), 7.73 (d, J = 8.0 Hz, 1H), 7.65 (d, J = 8.0 Hz, 1H), 7.53 (ddd, J = 7.6, 4.8, 0.8 Hz, 1H), 7.34-7.28 (m, 2H). Mass, EI-mass: calcd *m/z*: 195.08 u; found: 195 u.

1-methyl-2-(pyridin-2-yl)benzimidazole (L1)

2-(2-Pyridyl)benzimidazole (a) (1.95 g, 0.01 mol) and K₂CO₃ (2.07 g, 0.015 mol) were dissolved in DMF (20 mL) and stirred for 30 min; iodomethane (1.70 g, 0.012 mol) was added to the reaction mixture that was then stirred near 295 K for 4 h. After the solvent was evaporated under reduced pressure, H₂O (50 mL) and ethyl ethanoate (50 mL) were added. The organic layer was separated and dried over MgSO₄. The crude product was purified on a column chromatograph (silica gel) with a mixture of ethyl ethanoate and hexane (1/10) as eluent (1.49 g, 72.0 %). ¹H-NMR (DMSO-d₆): 8.76 (d, J = 4.0 Hz, 1H), 8.31 (d, J = 7.6 Hz, 1H), 8.01 (ddd, J = 8.0, 8.0, 1.6 Hz, 1H), 7.73 (d, J = 8.0 Hz, 1H), 7.65 (d, J = 8.0 Hz, 1H), 7.53 (ddd, J = 7.6, 4.8, 0.8 Hz, 1H), 7.34-7.28 (m, 2H), 4.24 (s, 3H). Mass, EI-mass: calcd *m/z*: 209.10 u; found: 208 u.

1-benzyl-2-(pyridin-2-yl)benzimidazole (L5)

2-(2-Pyridyl)benzimidazole (a) (1.95 g, 0.01 mol) and K₂CO₃ (2.07 g, 0.015 mol)

were dissolved in DMF (20 mL) and stirred for 30 min; (bromomethyl)benzene (2.04 g, 0.012 mol) was added to the reaction mixture that was then stirred near 295 K for 4 h. After evaporation of the solvent under reduced pressure, H₂O (50 mL) and ethyl ethanoate (50 mL) were added. The organic layer was separated and dried over MgSO₄. The crude product was purified on a column chromatograph (silica gel) with a mixture of ethyl ethanoate and hexane (1/10) as an eluent (2.20 g, 77.3 %). ¹H-NMR (DMSO-d₆): 8.70 (d, J = 4.0 Hz, 1H), 8.38 (d, J = 7.6 Hz, 1H), 8.01 (ddd, J = 8.0, 8.0, 1.6 Hz, 1H), 7.75 (m, 1H), 7.56 (m, 1H), 7.51 (m, 1H), 7.29-7.13 (m, 7H), 6.23 (s, 2H). Mass, EI-mass: calcd *m/z*: 285.13 u; found: 284 u.

1-decyl-2-(pyridin-2-yl)benzimidazole (L10)

2-(2-Pyridyl)benzimidazole (a) (1.95 g, 0.01 mol) and K₂CO₃ (2.07 g, 0.015 mol) were dissolved in DMF (20 mL) and stirred for 30 min; 1-bromodecane (2.04 g, 0.012 mol) was added into the reaction mixture that was then stirred near 295 K for 4 h. After evaporation of the solvent under reduced pressure, H₂O (50 mL) and ethyl ethanoate (50 mL) were added. The organic layer was separated and dried over MgSO₄. The crude product was purified on a column chromatograph (silica gel) with a mixture of ethyl ethanoate and hexane (1/10) as eluent (2.50 g, 74.5 %). ¹H-NMR (DMSO-d₆): 8.73 (d, J = 4.0 Hz, 1H), 8.34 (d, J = 7.6 Hz, 1H), 7.98 (ddd, J = 8.0, 8.0, 1.6 Hz, 1H), 7.73 (d, J = 8.0 Hz, 1H), 7.65 (d, J = 8.0 Hz, 1H), 7.51 (m, 1H), 7.34-7.26(m, 2H), 4.87 (t, 2H), 1.76 (m, 2H), 1.23 (m, 14H), 0.82 (t, 3H). Mass, EI-mass: calcd *m/z*: 335.24 u; found: 335 u.

2,2'-Bisbenzimidazole (b)

To a cooled (0 °C) solution of 1,2-benzenediamine (5.32 g, 0.02 mol) in a 50 mL round-bottomed flask was added dropwise hexachloropropanone (1.06 g, 0.002 mol) in ethandiol (5 mL) was sonicated for 1 h. The gray white precipitates were collected (78 %, 0.73 g). ¹H-NMR (DMSO-d₆): 7.90 (m, 4H), 7.30 (m, 4H). Mass, EI-mass: calcd *m/z*:

234.09 u ; found: 234 u.

1,1'-dimethyl-2,2'-bibenzimidazole (L11)

2,2'-Bisbenzimidazole (b) (0.468 g, 0.002 mol) and K₂CO₃ (0.69 g, 0.005 mol) were dissolved in DMF (20 mL) and stirred for 30 min; 1-iodomethane (2.04 g, 0.012 mol) was added into the reaction mixture that was then stirred near 295 K for 4 h. After evaporation of the solvent under reduced pressure, H₂O (50 mL) and ethyl ethanoate (50 mL) were added. The organic layer was separated and dried over MgSO₄. The crude product was purified on a column chromatography (silica gel) with a mixture of ethyl ethanoate and hexane (1/10) as eluent (0.352 g, 67.2 %). ¹H-NMR (DMSO-d₆): 7.90 (m, 4H), 7.30 (m, 4H), 4.28 (s, 6H). EI-mass: calcd *m/z*: 262.12 u ; found: 261 u.

Ruthenium Complexes

[Ru(4,4'-dicarboxylic-2,2'-bipyridine)(1-methyl-2-(pyridine-2-yl)benzimidazole)NCS₂] – RD1

In a typical one-pot synthesis, [RuCl₂ (p-cymene)]₂ (108 mg, 0.176 mmol) was dissolved in DMF (20 mL) and the precursor ligand L1 (73.6 mg, 0.352 mmol) was added. The reaction mixture was heated at 80 °C under argon for 4 h; then dcbpy (86 mg, 0.352 mmol) was added. The reaction mixture was refluxed at 140 °C for another 4 h in dark to avoid photoinduced cis-to-trans isomerization. Excess KNCS was added to the reaction mixture that was heated at 140 °C for 5 h. After the reaction, the solvent was removed with a rotary evaporator. Water was added to the resulting mixture to remove excess KNCS. The water-insoluble product was then collected on a sintered-glass crucible with suction filtration, washed with distilled water followed by diethyl ether, and dried in air. The crude product was dissolved in methanol then passed through a

Sephadex LH-20 column with methanol as eluent. The main band was collected and concentrated. This purification was repeated five times. A few drops of HNO₃ (aq, 0.01M) were added to precipitate the brown red product (91 mg, 38.5 %). Elemental analysis (%) calcd for C₂₇H₁₉N₇O₄S₂Ru·H₂O·2CH₃OH: C 46.27, H 3.88, N 13.02; found: C 46.10, H 3.87, N 12.78. Mass, LRMS (FAB): calcd *m/z*: 671.0 u; found: 671.0 u.

[Ru(4,4'-dicarboxylic-2,2'-bipyridine)(1-benzyl-2-(pyridin-2-yl)benzimidazole)NCS₂] – RD5

According to the same procedure as for **RD1**, but ligand L5 (75 mg, 0.352 mmol) was used instead of L1, resulting in a red brown powder (117 mg, 44.6 %). Elemental analysis (%) calcd for C₂₇H₁₉N₇O₄S₂Ru·CH₃OH·0.5TBAOH: C 54.31, H 5.18, N 11.88; found: C 54.70, H 5.02, N 11.62. Mass, LRMS (FAB): calcd *m/z*: 745.0 u; found: 745.0 u.

[Ru(4,4'-dicarboxylic-2,2'-bipyridine)(1-decyl-2-(pyridin-2-yl)benzimidazole)NCS₂] – RD10

According to the same procedure as for **RD1**, but ligand L10 (118 mg, 0.352 mmol) was used instead of L1, resulting in a red brown powder (132 mg, 47.1%). Elemental analysis (%) calcd for C₂₇H₁₉N₇O₄S₂Ru·2CH₃OH: C 53.01, H 5.27, N 11.39; found: C 53.02, H 5.24, N 11.24. Mass, LRMS (FAB): calcd *m/z*: 796.0 u; found: 796.0 u.

[Ru(4,4'-dicarboxylic-2,2'-bipyridine)(1,1'-dimethyl-2,2'-bibenzimidazole)NCS₂] – RD11

According to the same procedure as for **RD1**, but ligand L11 (100 mg, 0.352 mmol) was used instead of L1, resulting in a red purple powder (87 mg, 34.2 %). Elemental analysis (%) calcd for C₂₇H₁₉N₇O₄S₂Ru·H₂O·2CH₃OH: C 47.63, H 4.00, N 13.91; found: C 47.32, H 3.89, N 13.78. Mass, LRMS (FAB): calcd *m/z*: 722.0 u; found: 722.0 u.

Electrochemical measurements

Electrochemical tests were performed with a three-electrode potentiostat (CH Instruments, Model 750A) in dry DMF in the presence of $(n\text{-C}_4\text{H}_9)_4\text{NPF}_6$ (0.1 M). For cyclic voltammetry a three-electrode cell was equipped with a platinum (0.02 cm^2) disk as working electrode, a platinum wire as auxiliary electrode, and an Ag wire as reference electrode. Potentials are reported vs Ag wire with reference to a ferrocene/ferrocenium (Fc/Fc^+).

Electrode preparation and device fabrication

Photoanodes composed of nanocrystalline TiO_2 were prepared using the sol-gel method reported elsewhere.^{s2} A paste composed of TiO_2 particles ($\sim 15\text{ nm}$) for the transparent active layer was coated on a TiCl_4 -treated FTO glass substrate (FTO, $8\ \Omega/\square$) with repetitive screen printing to obtain the required film thickness. To improve the performance of DSSC, one additional scattering layer (particle size 200-600 nm) was screen-printed on the transparent active layer. The TiO_2 working electrodes were gradually heated according to a programmed procedure: (1) heating at $80\text{ }^\circ\text{C}$ for 15 min; (2) heating at $135\text{ }^\circ\text{C}$ for 10 min; (3) heating at $325\text{ }^\circ\text{C}$ for 30 min; (4) heating at $375\text{ }^\circ\text{C}$ for 5 min; (5) heating at $450\text{ }^\circ\text{C}$ for 15 min; (6) heating at $500\text{ }^\circ\text{C}$ for 15 min. The resulting layer had a transparent layer (thickness 3-12 μm) and a scattering layer (thickness $\sim 3\ \mu\text{m}$), which were treated again with TiCl_4 at $70\text{ }^\circ\text{C}$ for 30 min and sintered at $500\text{ }^\circ\text{C}$ for 30 min. After cooling in air, the sintered TiO_2 films were immersed in dye solutions (0.3 mM in anhydrous $\text{CH}_3\text{CN}/t\text{-BuOH}$ (1:1 v/v) at $25\text{ }^\circ\text{C}$ for 3 h) containing CDCA (0.3 mM) for dye loading onto the working electrodes. The counter electrode was made on spin-coating the H_2PtCl_6 /isopropanol solution onto a FTO glass substrate (FTO, $8\ \Omega/\square$, typical size $1.0 \times 1.5\text{ cm}^2$) through thermal decomposition at $380\text{ }^\circ\text{C}$ for

30 min. The two electrodes were assembled into a cell of sandwich type and sealed with a hot-melt film (SX1170, thickness 25 μm). The electrolyte solution for all devices contains 1-butyl-3-methyl-imidazolium iodide (BMII, 1.0 M), guanidinium thiocyanate (0.1 M), LiI (0.05 M), I_2 (0.03 M) and 4-*t*-butylpyridine (TBP, 0.5 M) in a solvent mixture containing acetonitrile and valeronitrile (volume ratio 85:15).^{s3}

Dye-loading examination

To determine the dye-loading amounts of **RD1**, **RD5**, **RD10**, **RD11** and **N719** on TiO_2 films, the dye was desorbed in tetrabutylammonium hydroxide (0.1 M, TBAOH) in DMF (2 mL). The absorption spectrum of the solution was recorded with a UV-vis spectrometer. A calibration curve for dyes in TBAOH in DMF (0.1 M) was derived to obtain the absorption coefficient. The amounts of dye coverage on TiO_2 films were obtained from the measured absorbances in the spectra (cuvette thickness 3 mm) and the calibrated absorption coefficient of dyes according to Beers' law.

Photovoltaic characterization

The current-voltage characteristics were determined with a digital source meter (Keithley 2400) with the device under one-sun AM 1.5 irradiation from a solar simulator (XES-502S, SAN-EI) calibrated with a standard silicon reference cell (Oriel PN 91150V, VLSI standards). When the device is irradiated with the solar simulator, the source meter sends a voltage (V) to the device, and the photocurrent (I) is read at each step controlled with a computer via a GPIB interface. The efficiency (η) of conversion of light to electricity is obtained with this formula, $\eta = J_{\text{SC}} V_{\text{OC}} FF / P_{\text{in}}$, in which $J_{\text{SC}}/\text{mA cm}^{-2}$ is the current density measured at short circuit, and V_{OC}/V is the voltage measured at open circuit. P_{in} is the input radiation power (for one-sun illumination $P_{\text{in}} =$

100 mW cm⁻²) and *FF* is the filling factor. For all measurements, the DSSC devices were covered with a black mask (aperture area 0.16 cm²) to ensure that the measured photocurrent was not exaggerated. The spectra of the IPCE of the corresponding devices were obtained with a system comprising a Xe lamp (PTi A-1010, 150 W), a monochromator (Dongwoo DM150i, 1200 gr/mm blazed at 500 nm), and a source meter (Keithley 2400). A standard Si photodiode (ThorLabs FDS1010) served as reference to calibrate the power density of the light source at each wavelength. Both photocurrent densities of the target device and the reference Si cell were measured under the same experimental conditions (excitation beam size ~0.08 cm²) so to obtain the efficiency of the device from a comparison of the current ratio and the value of the reference cell at each wavelength.^{s4}

Photocurrent and photovoltage decay measurements

The photocurrent and photovoltage decays were obtained using the instrumental setup reported elsewhere.^{s5} The devices comprising **RD1**, **RD5**, **RD10** and **RD11** were irradiated from the counter-electrode side with a weak pulse (~1 μJ pulse⁻¹) from a laser (NT342, EKSPLA, pulse duration ~8 ns) at 430 nm under background (bias) illumination with a CW He-Ne laser (λ= 632.8 nm). The intensity of the bias light was varied in eleven steps using neutral density filters. The resulting photocurrent and photovoltage transients were recorded on a digital oscilloscope (LeCroy 9350); the signals passed a current preamplifier (SR570, SRC) at a short-circuit condition and a voltage preamplifier (SR560, SRC) at an open-circuit condition.

Ultrarapid Transient Infrared Absorption Spectroscopy

We measured transient absorption were performed with a conventional

pump-probe method reported elsewhere.^{s6} The laser pulses were amplified with a regenerative amplifier (Legend-USP-1K-He, Coherent) seeded with a mode-locked Ti:sapphire laser system (Mantis-Seed/Verdi V5, Coherent) and pumped with a Nd:YLF laser (Evolution 30, Coherent, 1 kHz). This system produces pulses of duration ~40 fs centered at 800 nm and with average energy 2.5 mJ pulse⁻¹. The output pulse (800 nm) was split into two parts to generate pump and probe beams. One part was directed into an optical parametric amplifier (OPerA-F, Coherent) to generate the tunable near-IR pulses from 1.1 to 2.5 μm , followed by frequency mixing in an AgGaS₂ crystal to generate a mid-IR probe beam tunable from 3 to 10 μm with a bandwidth ~130 cm⁻¹ at 4.9 μm . The other part was used to generate a pump beam at 625 nm by second harmonic generation (SHG) of another OPA output at 1.3 μm . The IR probe was separated into two parts for use as sample and reference pulses; the pump pulse overlaps with only the sample probe pulse. This probe pulse (centered at 2100 cm⁻¹) after passing through the sample was dispersed in a spectrometer (Micro HR motorized, Jobin-Yvon Horiba) with a detector MCT array detector (IR6416, Infrared Systems Development Corp) to yield resolution 21 nm (9.3 cm⁻¹ at 2100 cm⁻¹). Every alternate pump pulse was blocked with a synchronized chopper (MC1000A, Thorlabs) at 500 Hz; the absorbance change was calculated from sequential pump versus un-pumped probe pulses. The instrument response function (IRF) and zero time delay were determined with a thin Si wafer, which gives an instantaneous mid-IR absorption response after excitation at 625 nm. The IRF was characterized with a Gaussian function of full width 160 fs at half maximum (fwhm).

References

- s1 A. Islam, H. Sugihara and H. Arakawa, *Journal of Photochemistry and*

Photobiology A: Chemistry, 2003, **158**, 131.

- s2 (a) S. Ito, P. Chen, P. Comte, M. K. Nazeeruddin, P. Liska, P. Péchy and M. Grätzel, *Prog. Photovolt: Res. Appl.*, 2007, **15**, 603; (b) S. Ito, T. N. Murakami, P. Comte, P. Liska, C. Grätzel, M. K. Nazeeruddin and M. Grätzel, *Thin Solid Films*, 2008, **516**, 4613.
- s3 F. Gao, Y. Wang, D. Shi, J. Zhang, M. Wang, X. Jing, R. Humphry-Baker, P. Wang, S. M. Zakeeruddin and M. Grätzel, *J. Am. Chem. Soc.*, 2008, **130**, 10720.
- s4 C.-C. Chen, H.-W. Chung, C.-H. Chen, H.-P. Lu, C.-M. Lan, S.-F. Chen, L. Luo, C.-S. Hung and E. W.-G. Diau, *J. Phys. Chem. C*, 2008, **112**, 19151.
- s5 (a) L. Luo, C.-J. Lin, C.-Y. Tsai, H.-P. Wu, L.-L. Li, C.-F. Lo, C.-Y. Lin and E. W.-G. Diau, *Phys. Chem. Chem. Phys.*, 2010, **12**, 1064; (b) L. Luo, C.-J. Lin, C. S. Hung, C.-F. Lo, C.-Y. Lin and E. W.-G. Diau, *Phys. Chem. Chem. Phys.*, 2010, in press (DOI: 10.1039/C0CP00458H).
- s6 C.-W. Chang, L. Luo, C. K. Chou, C.-F. Lo, C.-Y. Lin, C.-S. Hung, Y.-P. Lee and E. W.-G. Diau, *J. Phys. Chem. C*, 2009, **113**, 11524.